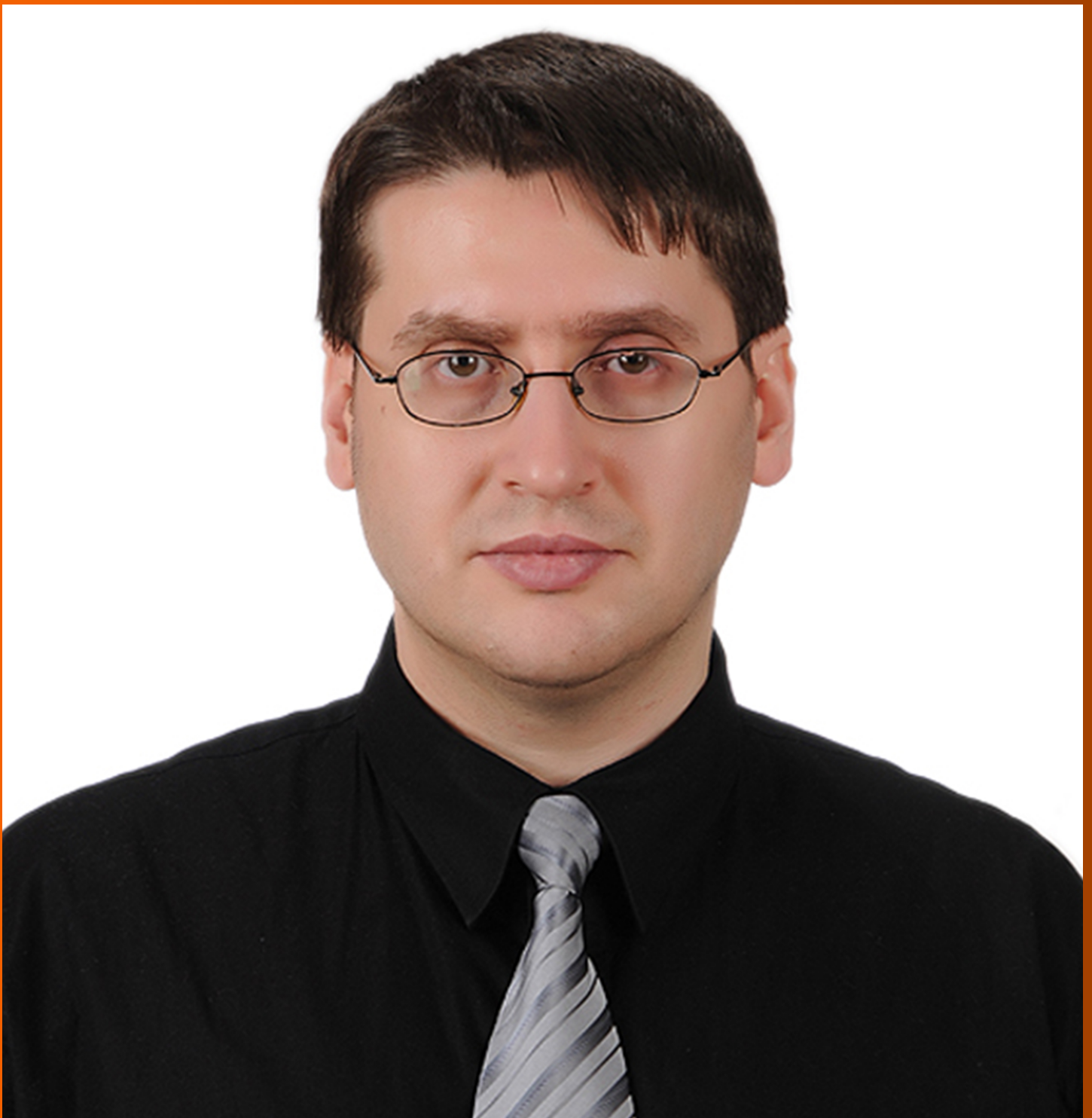


World Journal of *Gastroenterology*

World J Gastroenterol 2021 September 7; 27(33): 5460-5624



THERAPEUTIC AND DIAGNOSTIC GUIDELINES

- 5460 Guidelines on postoperative magnetic resonance imaging in patients operated for cryptoglandular anal fistula: Experience from 2404 scans
Garg P, Kaur B, Yagnik VD, Dawka S, Menon GR

REVIEW

- 5474 Neutrophil extracellular traps in gastrointestinal cancer
Chu ZQ, Zhang KC, Chen L
- 5488 Microbiota and viral hepatitis: State of the art of a complex matter
Milosevic I, Russo E, Vujovic A, Barac A, Stevanovic O, Gitto S, Amedei A
- 5502 Clinical perspectives, assessment, and mechanisms of metabolic-associated fatty liver disease in patients with COVID-19
Campos-Murguía A, Román-Calleja BM, González-Regueiro JA, Hurtado-Díaz-de-León I, Solís-Ortega AA, Flores-García NC, García-Juárez I, Ruiz-Margáin A, Macías-Rodríguez RU

MINIREVIEWS

- 5520 Impact of COVID-19 on inflammatory bowel disease practice and perspectives for the future
Viganò C, Mulinacci G, Palermo A, Barisani D, Pirola L, Fichera M, Invernizzi P, Massironi S
- 5536 Surveillance for hepatocellular carcinoma in chronic viral hepatitis: Is it time to personalize it?
Demirtas CO, Brunetto MR
- 5555 Gut microbiota-derived metabolites as key mucosal barrier modulators in obesity
Wei YX, Zheng KY, Wang YG

ORIGINAL ARTICLE**Basic Study**

- 5566 Adiponectin and the regulation of gastric content volume in the newborn rat
Wang H, Esemu-Ezewu P, Pan J, Ivanovska J, Gauda EB, Belik J
- 5575 Characterization of gut microbiome and metabolome in *Helicobacter pylori* patients in an underprivileged community in the United States
White B, Sterrett J, Grigoryan Z, Lally L, Heinze J, Alikhan H, Lowry C, Perez LJ, DeSipio J, Phadtare S

Retrospective Study

- 5595 Gastric cancer mortality related to direct radiographic and endoscopic screening: A retrospective study
Hagiwara H, Moki F, Yamashita Y, Saji K, Iesaki K, Suda H

5610 Radiomics for predicting perineural invasion status in rectal cancer

Li M, Jin YM, Zhang YC, Zhao YL, Huang CC, Liu SM, Song B

LETTER TO THE EDITOR

5622 Comment on “Diagnostic approach to faecal incontinence: What test and when to perform?”

Wang JT, Miao YD, Guan QL

ABOUT COVER

Editorial Board Member of *World Journal of Gastroenterology*, Güray Can, MD, Associate Professor, Chief, Department of Gastroenterology, Bolu İzzet Baysal Education and Research Hospital, Bolu Abant İzzet Baysal University, Gölköy Campus, Bolu 14030, Turkey. guraycan@ibu.edu.tr

AIMS AND SCOPE

The primary aim of *World Journal of Gastroenterology* (WJG, *World J Gastroenterol*) is to provide scholars and readers from various fields of gastroenterology and hepatology with a platform to publish high-quality basic and clinical research articles and communicate their research findings online. WJG mainly publishes articles reporting research results and findings obtained in the field of gastroenterology and hepatology and covering a wide range of topics including gastroenterology, hepatology, gastrointestinal endoscopy, gastrointestinal surgery, gastrointestinal oncology, and pediatric gastroenterology.

INDEXING/ABSTRACTING

The WJG is now indexed in Current Contents®/Clinical Medicine, Science Citation Index Expanded (also known as SciSearch®), Journal Citation Reports®, Index Medicus, MEDLINE, PubMed, PubMed Central, and Scopus. The 2021 edition of Journal Citation Report® cites the 2020 impact factor (IF) for WJG as 5.742; Journal Citation Indicator: 0.79; IF without journal self cites: 5.590; 5-year IF: 5.044; Ranking: 28 among 92 journals in gastroenterology and hepatology; and Quartile category: Q2. The WJG's CiteScore for 2020 is 6.9 and Scopus CiteScore rank 2020: Gastroenterology is 19/136.

RESPONSIBLE EDITORS FOR THIS ISSUE

Production Editor: *Ying-Yi Yuan*; Production Department Director: *Xiang Li*; Editorial Office Director: *Ze-Mao Gong*.

NAME OF JOURNAL

World Journal of Gastroenterology

ISSN

ISSN 1007-9327 (print) ISSN 2219-2840 (online)

LAUNCH DATE

October 1, 1995

FREQUENCY

Weekly

EDITORS-IN-CHIEF

Andrzej S Tarnawski, Subrata Ghosh

EDITORIAL BOARD MEMBERS

<http://www.wjgnet.com/1007-9327/editorialboard.htm>

PUBLICATION DATE

September 7, 2021

COPYRIGHT

© 2021 Baishideng Publishing Group Inc

INSTRUCTIONS TO AUTHORS

<https://www.wjgnet.com/bpg/gerinfo/204>

GUIDELINES FOR ETHICS DOCUMENTS

<https://www.wjgnet.com/bpg/GerInfo/287>

GUIDELINES FOR NON-NATIVE SPEAKERS OF ENGLISH

<https://www.wjgnet.com/bpg/gerinfo/240>

PUBLICATION ETHICS

<https://www.wjgnet.com/bpg/GerInfo/288>

PUBLICATION MISCONDUCT

<https://www.wjgnet.com/bpg/gerinfo/208>

ARTICLE PROCESSING CHARGE

<https://www.wjgnet.com/bpg/gerinfo/242>

STEPS FOR SUBMITTING MANUSCRIPTS

<https://www.wjgnet.com/bpg/GerInfo/239>

ONLINE SUBMISSION

<https://www.f6publishing.com>

Retrospective Study

Radiomics for predicting perineural invasion status in rectal cancer

Mou Li, Yu-Mei Jin, Yong-Chang Zhang, Ya-Li Zhao, Chen-Cui Huang, Sheng-Mei Liu, Bin Song

ORCID number: Mou Li 0000-0002-7101-5942; Yu-Mei Jin 0000-0001-6606-8049; Yong-Chang Zhang 0000-0003-0402-2525; Ya-Li Zhao 0000-0002-8895-1972; Chen-Cui Huang 0000-0003-3307-6872; Sheng-Mei Liu 0000-0003-4575-0799; Bin Song 0000-0002-7269-2101.

Author contributions: Song B and Li M designed the research; Jin YM and Liu SM collected the data; Li M, Zhang YC, Zhao YL, and Huang CC analyzed the data; Li M and Song B wrote the paper; all authors have read and approved the final manuscript.

Institutional review board

statement: This study was reviewed and approved by the Ethics Committee of West China Hospital of Sichuan University (Approved No.1159).

Informed consent statement:

Patients were not required to give informed consent to the study because the analysis used anonymous clinical data that were obtained after each patient agreed to treatment by written consent.

Conflict-of-interest statement: Zhao YL and Huang CC are employed by the company Beijing Deepwise & League of PHD Technology Co., Ltd. The remaining authors declare no conflicts-of-interest related to this article.

Mou Li, Yu-Mei Jin, Sheng-Mei Liu, Bin Song, Department of Radiology, West China Hospital of Sichuan University, Chengdu 610041, Sichuan Province, China

Yong-Chang Zhang, Department of Radiology, Chengdu Seventh People's Hospital, Chengdu 610213, Sichuan Province, China

Ya-Li Zhao, Chen-Cui Huang, Department of Research Collaboration, R&D Center, Beijing Deepwise & League of PHD Technology Co., Ltd, Beijing 100080, China

Corresponding author: Bin Song, MD, Chief Doctor, Professor, Department of Radiology, West China Hospital of Sichuan University, No. 37 Guoxue Alley, Chengdu 610041, Sichuan Province, China. songlab_radiology@163.com

Abstract**BACKGROUND**

Perineural invasion (PNI), as a key pathological feature of tumor spread, has emerged as an independent prognostic factor in patients with rectal cancer (RC). The preoperative stratification of RC patients according to PNI status is beneficial for individualized treatment and improved prognosis. However, the preoperative evaluation of PNI status is still challenging.

AIM

To establish a radiomics model for evaluating PNI status preoperatively in RC patients.

METHODS

This retrospective study enrolled 303 RC patients in a single institution from March 2018 to October 2019. These patients were classified as the training cohort ($n = 242$) and validation cohort ($n = 61$) at a ratio of 8:2. A large number of intra- and peritumoral radiomics features were extracted from portal venous phase images of computed tomography (CT). After deleting redundant features, we tested different feature selection ($n = 6$) and machine-learning ($n = 14$) methods to form 84 classifiers. The best performing classifier was then selected to establish Rad-score. Finally, the clinicoradiological model (combined model) was developed by combining Rad-score with clinical factors. These models for predicting PNI were compared using receiver operating characteristic curve (ROC) analysis and area under the ROC curve (AUC).

RESULTS

One hundred and forty-four of the 303 patients were eventually found to be PNI-

Data sharing statement: No additional data are available.

Open-Access: This article is an open-access article that was selected by an in-house editor and fully peer-reviewed by external reviewers. It is distributed in accordance with the Creative Commons Attribution NonCommercial (CC BY-NC 4.0) license, which permits others to distribute, remix, adapt, build upon this work non-commercially, and license their derivative works on different terms, provided the original work is properly cited and the use is non-commercial. See: <http://creativecommons.org/licenses/by-nc/4.0/>

Manuscript source: Unsolicited manuscript

Specialty type: Gastroenterology and hepatology

Country/Territory of origin: China

Peer-review report's scientific quality classification

Grade A (Excellent): 0
Grade B (Very good): B
Grade C (Good): C
Grade D (Fair): 0
Grade E (Poor): 0

Received: June 2, 2021

Peer-review started: June 2, 2021

First decision: June 25, 2021

Revised: July 3, 2021

Accepted: August 11, 2021

Article in press: August 11, 2021

Published online: September 7, 2021

P-Reviewer: Dulskas A, Peltrini R

S-Editor: Liu M

L-Editor: A

P-Editor: Guo X



positive. Clinical factors including CT-reported T stage (cT), N stage (cN), and carcinoembryonic antigen (CEA) level were independent risk factors for predicting PNI preoperatively. We established Rad-score by logistic regression analysis after selecting features with the L1-based method. The combined model was developed by combining Rad-score with cT, cN, and CEA. The combined model showed good performance to predict PNI status, with an AUC of 0.828 [95% confidence interval (CI): 0.774-0.873] in the training cohort and 0.801 (95%CI: 0.679-0.892) in the validation cohort. For comparison of the models, the combined model achieved a higher AUC than the clinical model (cT + cN + CEA) achieved ($P < 0.001$ in the training cohort, and $P = 0.045$ in the validation cohort).

CONCLUSION

The combined model incorporating Rad-score and clinical factors can provide an individualized evaluation of PNI status and help clinicians guide individualized treatment of RC patients.

Key Words: Radiomics; Perineural invasion; Rectal cancer; Computed tomography; Preoperative prediction; Model building

©The Author(s) 2021. Published by Baishideng Publishing Group Inc. All rights reserved.

Core Tip: In this study, a radiomics model integrating Rad-score and clinical factors was developed and validated for predicting perineural invasion status in patients with rectal cancer. Radiomics features were extracted from intra- and peritumoral regions. This radiomics model showed good performance and outperformed the clinical factors. Therefore, the combined model might assist in predicting perineural invasion status and improving prognosis of patients with rectal cancer.

Citation: Li M, Jin YM, Zhang YC, Zhao YL, Huang CC, Liu SM, Song B. Radiomics for predicting perineural invasion status in rectal cancer. *World J Gastroenterol* 2021; 27(33): 5610-5621

URL: <https://www.wjgnet.com/1007-9327/full/v27/i33/5610.htm>

DOI: <https://dx.doi.org/10.3748/wjg.v27.i33.5610>

INTRODUCTION

Rectal cancer (RC) is one of the most common cancers of the digestive tract worldwide, with a growing morbidity[1]. In the last decade, the combination of neoadjuvant chemoradiotherapy (nCRT) and surgery has improved local control of locally advanced RC, but it does not significantly affect prognosis[2]. Different biological characteristics of RC may cause different treatment responses, risks of distant metastasis, and outcomes[3].

Recently, there is an increasing interest in perineural invasion (PNI) as a potential route of tumor spread, in addition to the well-known routes of direct extension, lymphatic metastasis, and hematogenous metastasis[4]. PNI refers to the biological process characterized by cancer cells invading the nerves and spreading along the nerve sheaths[5,6]. This process can be found in the main tumor and peritumoral area [7,8]. Previous studies have demonstrated the prognostic value of PNI in RC in terms of both recurrence and survival[9-11]. Other studies have shown that PNI can be an indicator for identifying patients who can benefit from nCRT and postoperative adjuvant chemotherapy[12,13]. Therefore, understanding PNI status in advance is helpful for clinicians to make individualized treatment plans for RC patients.

However, PNI status can only be confirmed by assessing the pathology of surgical specimens. In other words, neither biopsy nor imaging examinations [computed tomography (CT)/magnetic resonance imaging (MRI)] can accurately determine PNI status of RC[6]. Recent advances in radiomics have enabled researchers to extract numerous quantitative features from medical images and provide a comprehensive overview of heterogeneity in tumors[14]. Latterly, radiomics analysis has been used to predict PNI status in colorectal cancer[14,15]. Considering the higher incidence of PNI

in RC (compared with colon cancer)[16], several researchers evaluated the performance of MRI-based radiomics for PNI prediction in RC[6,17,18]. However, the sample sizes in the previous studies were really small (PNI+: 26-32). At present, there is still a lack of CT-based radiomics research in this field. Therefore, we aimed to evaluate the predictive value of CT-based radiomics for PNI prediction in a bigger cohort of RC patients.

MATERIALS AND METHODS

Patients

The local ethics committee approved this study (document number: 1159), and the requirement of informed consent was waived because of the retrospective nature of this study.

The RC patients were reviewed by browsing the radiological and pathological databases from March 2018 to October 2019. A total of 303 patients (170 men and 133 women, mean age 58.9 ± 11.7 years, age range 23-86 years) were enrolled, according to the following inclusion criteria: (1) Adults with histologically confirmed rectal adenocarcinoma; (2) Clinical materials such as enhanced CT images and tumor markers were complete; and (3) No prior therapy before CT examination. The exclusion criteria were as follows: (1) Quality of CT images was poor; (2) Patients treated without surgery; and (3) Patients with other malignant tumors besides RC. The patient recruitment pathway is shown in [Figure 1](#). The workflow of the radiomics analysis is shown in [Figure 2](#).

The clinical and pathological data of each patient were derived from medical records. The baseline data including age, sex, tumor volume, location, tumor markers [carcinoembryonic antigen (CEA), carbohydrate antigen (CA) 19-9, and CA125], pathological TNM stage, and histological grade are shown in [Table 1](#).

Reference standard for pathology

All patients with RC were diagnosed by pathology based on resected specimens. The pathological confirmatory reports were acquired from electronic medical records. PNI status was defined as positive, if (1) At least 33% of the nerve circumference was surrounded by cancer cells (without invasion of nerve sheath); or (2) Cancer cells were within any layer of the nerve sheath[6,19].

CT examination and evaluation

In our hospital, the chest-abdomen-pelvis enhanced CT is used to detect both primary and metastatic lesions for patients with clinically suspected RC. The CT scanners were restricted to Somatom Definition AS+ and Somatom Definition Flash in this study. The parameters of CT examinations are shown in the [Supplementary material](#).

Two experienced radiologists (10 years' and 5 years' experience in abdominal imaging) were assigned to review CT images. The identification of patients was removed from CT images, and the readers were blinded to all clinical and pathological information. The CT-reported T stage (cT) and N stage (cN) were determined by summarizing the results of the two readers ([Table 1](#)). The inter-observer variability of cT/cN was evaluated by a weighted kappa statistics test. Because CT is limited to distinguish T1 from T2 in RC, lesions of cT1 were classified as cT2 in this study. When reviewing the CT images, the radiologists solved disagreements by discussion.

Feature extraction and model building

The stability of radiomics features was tested on 20 patients. One radiologist drew volumes of interest (VOIs) twice for evaluating intra-class correlation coefficient (intra-ICC), and the other drew VOIs once for evaluating inter-ICC. The features with ICC < 0.75 were deleted according to the commonly admitted knowledge: ICC < 0.5, poor reliability; 0.5-0.75, moderate reliability; ICC > 0.75, good reliability[20]. The main tumor and peritumoral area were separately drawn slice by slice to obtain intra- and peritumoral features ([Figure 2](#)).

The CT images were resampled to a pixel spacing of 1.0 mm in three anatomical directions. Then high- and low-pass wavelet filters, Laplacian-of-Gaussian filters, and other transformation methods such as square, square root, logarithm, exponential, gradient, lbp2d, and lbp3 were used to pre-process the original images. Radiomics features were extracted by using PyRadiomics[21]. A total of 4214 features (three types: First-order statistics, shape features, and texture features) were extracted from

Table 1 Baseline characteristics of the study population

Characteristics	PNI ^a (n = 144)	PNI ^b (n = 159)	P value	The training set(n = 242)	The validation set(n = 61)	P value
Age (mean ± SD, yr)	58.9 ± 11.8	58.9 ± 11.7	0.952	58.4 ± 11.9	60.8 ± 10.2	0.162
Sex (male/female)	77/67	93/66	0.379	140/102	30/31	0.223
Volume (cm ³)	19.7	20.8	0.132	20.1	20.8	0.847
Location ¹			0.075			0.045
Middle-low	101	96		164	33	
High	43	63		78	28	
cT stage (T1-2/T3/T4)	25/98/21	57/90/12	< 0.001	61/156/25	21/32/8	0.222
cN stage (N0/N1/N2)	31/52/61	75/59/25	< 0.001	89/84/69	17/27/17	0.313
Neoadjuvant therapy (+/-)	25/119	37/122	0.203	51/191	11/50	0.599
CEA (+/-) (positive ≥ 5 ng/mL)	77/67	56/103	0.001	107/135	26/35	0.823
CA19-9 (+/-) (positive ≥ 30 U/mL)	43/101	35/124	0.119	64/178	14/47	0.577
CA125 (+/-) (positive ≥ 24 U/mL)	20/124	15/144	0.226	20/222	3/58	0.378
pT stage (T1/T2/T3/T4)	0/15/117/12	8/44/95/12	< 0.001	6/48/171/17	2/11/41/7	0.584
pN stage (0/N1/N2)	29/74/41	81/56/22	< 0.001	88/101/53	22/29/10	0.579
Stage (I/II/III)	10/28/115	38/43/78	< 0.001	40/48/154	8/14/39	0.731
Histologic grade (G1/G2/G3)	1/105/38	2/133/24	0.014	2/189/51	1/49/11	0.523
Rad-score	0.60 ± 0.19	0.40 ± 0.20	< 0.001	0.50±0.21	0.49 ± 0.23	0.805

¹Location: Low (0-5 cm from the anal verge), middle (5.1-10 cm from the anal verge), and high (10.1-15 cm from the anal verge). This table summarized the results of cT-stage and cN-stage for the two readers. CT: Computed tomography; PNI: Perineural invasion; CEA: Carcinoembryonic antigen; CA19-9: Carbohydrate antigen 19-9; CA125: Carbohydrate antigen 125; cT stage: Computed tomography-reported T stage; cN stage: Computed tomography-reported N stage; pT stage: Pathological T stage; pN stage: Pathological N stage.

intra- and peritumoral regions. Z-score was used to normalize the features for eliminating the differences in the value scales. Redundant features were randomly removed by correlation analysis with a threshold of 0.48. Then the features were selected using six different methods (analysis of variance, Pearson, mutual information, L1-based, tree-based, and recursive). Subsequently, 14 different machine-learning methods were used to build 84 classifiers. The optimal parameters were adjusted to improve the area under the receiver operating characteristic (ROC) curve (AUC) of the test set and output the best classifier (Rad-score).

Statistically significant risk variables (Rad-score and clinical factors) from the univariate logistic regression analysis were then entered into a multivariate analysis for developing the clinical and combined models. A nomogram was generated for the combined model visualization, graphical evaluation of variable importance, and the calculation of predictive accuracy. ROC curve analyses were performed to assess the diagnostic performance of the models.

Statistical analysis

All statistical analyses were performed using R software (version 3.6.1), SPSS (version 21), Stata (version 15.0), and Medcalc (version 15.2.2). Differences of the factors in Table 1 were assessed by chi-square test or Fisher's exact test, Mann-Whitney test, and t-test. AUCs of the models were compared by DeLong's test.

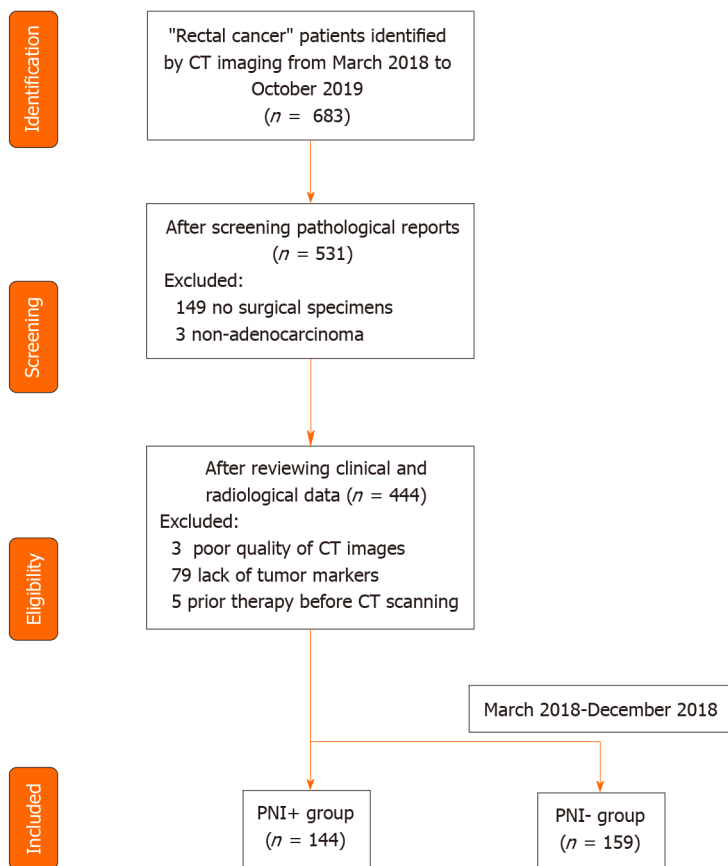


Figure 1 Flowchart of patients' recruitment pathway. CT: Computed tomography; PNI: Perineural invasion.

RESULTS

Patient characteristics

A total of 303 RC patients (144 PNI⁺ and 159 PNI⁻) were enrolled in this study. Clinical factors such as cT/cN stage, CEA (+/-), pathological T/N stage, and grade had significant differences between PNI⁺ and PNI⁻ groups (Table 1). The weighted kappa coefficients of cT and cN between two readers were 0.709 [95% confidence interval (CI): 0.630-0.789] and 0.849 (95%CI: 0.801-0.897), which showed substantial consistency for cT and almost perfect consistency for cN (0.41-0.60, moderate, 0.61-0.80, substantial and 0.81-1.00, almost perfect)[22]. There were no significant differences in sex, age, volume, location, CA19-9, and CA125 between PNI⁺ and PNI⁻ groups (Table 1). The patients were randomly divided into the training cohort ($n = 242$) and the validation cohort ($n = 61$). Except for location ($P = 0.045$), there were no significant differences in other factors between the training and validation groups (Table 1).

Feature selection and model building

A total of 3095 features (1490 intratumoral and 1605 peritumoral) had good reliability with ICC > 0.75. After deleting redundant features, we selected only seven intratumoral and 13 peritumoral features using the L1-based method. Rad-score was established by logistic regression, as shown in Supplementary material. Rad-score was an independent risk factor for predicting PNI [odds ratio (OR) = 3.148, $P < 0.001$]. As for clinical factors, CEA, cT, and cN were independent risk factors for predicting PNI preoperatively (OR = 2.528, 1.636, and 1.458; $P = 0.003$, 0.087, and 0.001, respectively), as shown in Table 2. The factor location had a significant difference in the univariate logistic regression analysis; however, it was excluded by multivariate analysis (Table 2). Thus, the combined model (Rad-score + CEA + cT + cN) was built by multivariate logistic regression analysis. The formula of the combined model is shown in Supplementary material.

A nomogram was generated for the visualization of the combined model (Figure 3). Higher total score obtained from the nomogram is associated with greater predicted risk of PNI. The combined model had good fit according to the Hosmer-Lemeshow test ($P = 0.122$). In the calibration curve of the nomogram (Figure 4), the y axis

Table 2 Risk factors selected by logistic regression analysis

Variables	Univariate		Multivariate	
	OR	P value	OR	P value
Age	1.001	0.961	-	-
Sex	0.787	0.358	-	-
Volume	1.000	1.000	-	-
Location	1.779	0.050	1.470	0.265
cT stage	2.328	< 0.001	1.636	0.087
cN stage	1.550	< 0.001	1.458	0.001
CEA	2.631	< 0.001	2.528	0.003
CA19-9	1.478	0.182	-	-
CA125	0.717	0.484	-	-
Rad-score	3.012	< 0.001	3.148	< 0.001

If *P* value < 0.1, variables were included in the model. CEA: Carcinoembryonic antigen; CA19-9: Carbohydrate antigen 19-9; CA125: Carbohydrate antigen 125; OR: Odds ratio.

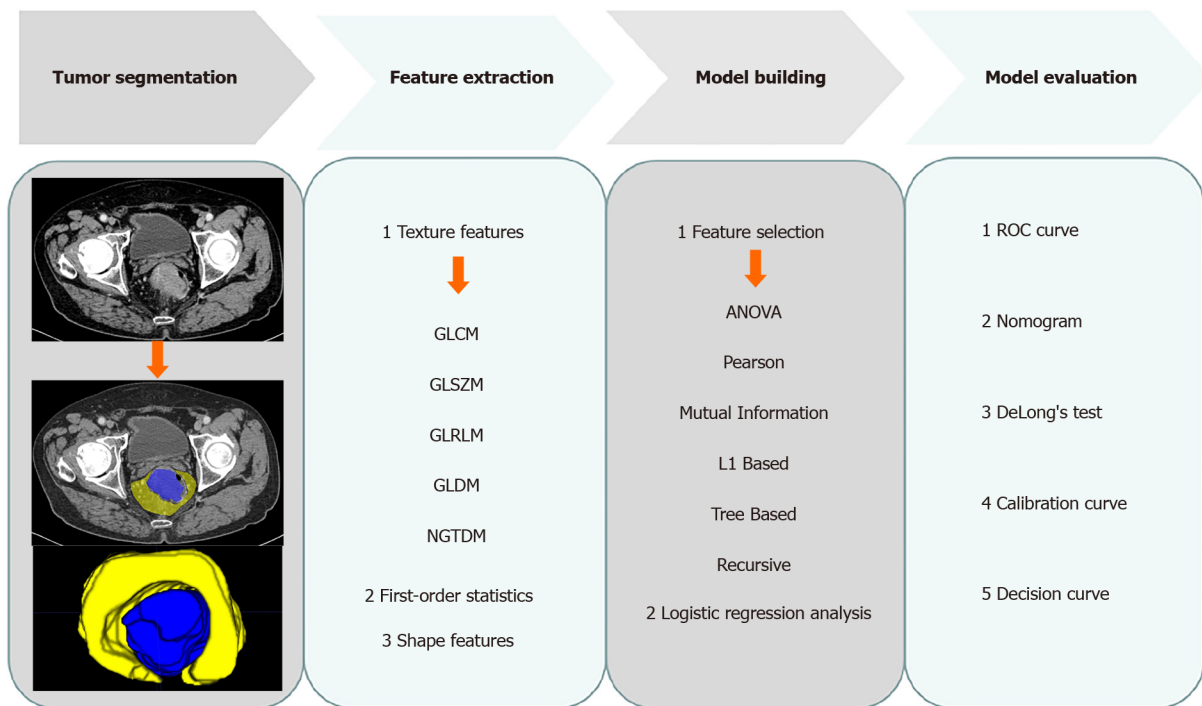


Figure 2 Radiomics workflow. GLCM: Gray level co-occurrence matrix; GLSZM: Gray level size zone matrix; GLRLM: Gray level run length matrix; GLDM: Gray level dependence matrix; NGTDM: Neighbouring gray tone difference matrix; ANOVA: Analysis of variance; ROC: Receiver operating characteristic curve.

represents the actual observed probability of PNI, and the x axis represents the predicted probability of PNI. A locally weighted regression line (solid line) of calibration plots is used to demonstrate the general trend of predicted risk. The model had a good agreement between the predicted and observed probability, because the solid line was close to the reference line (dotted line) in this study. This conclusion was consistent with the result of the Hosmer-Lemeshow test. However, among patients with predicted probability > 83%, the model overestimated actual risk of PNI[†] (about 15% at most). The decision curve was performed to assess the clinical usefulness of the combined model in predicting PNI. The net benefit is measured on the y axis. **Figure 4** shows that the combined model (nomogram) obtained more benefit than “treat all”, “treat none”, Rad-score, and the clinical model, when the threshold probability was

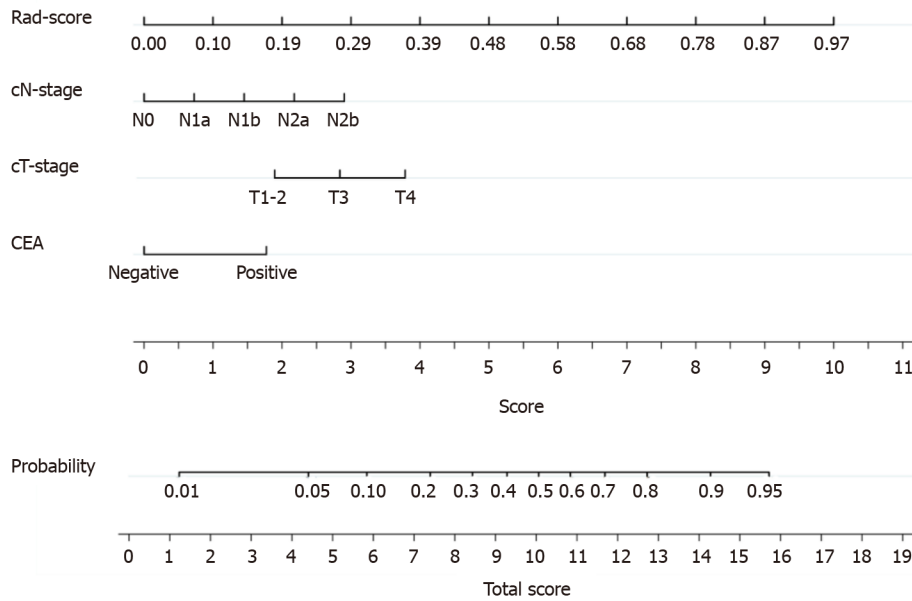


Figure 3 The nomogram was developed in the training cohort. Sum the points of variables in the “score” axis to get the total points. The risk of perineural invasion is the corresponding value on the “probability” axis. CEA: Carcinoembryonic antigen; cT: Computed tomography-reported T stage; cN: Computed tomography-reported N stage.

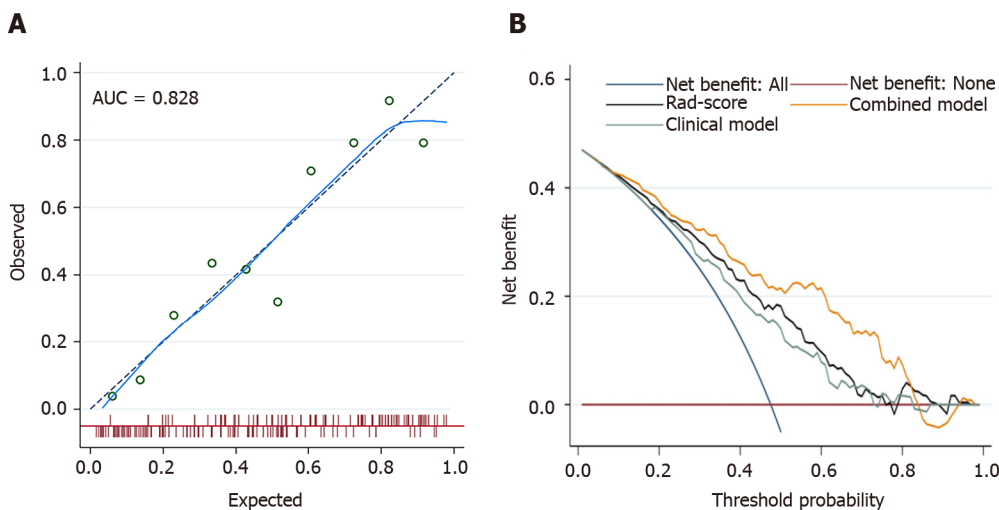


Figure 4 The fit and usefulness evaluation of the nomogram. A: The calibration curve of the nomogram shows a good agreement between the predicted and observed risks in the training cohort; B: The decision curve demonstrates that the nomogram (combined model) obtains more benefit than “treat all”, “treat none”, Rad-score, and the clinical model, when the threshold probability is in the range of 10% to 83%. AUC: Area under the receiver operating characteristic curve.

found to be in the range of 10% to 83%.

Classification results

In the case of the clinical model (cT + cN + CEA), the resulting AUCs were 0.718 (95%CI: 0.657-0.774) in the training cohort and 0.674 (95%CI: 0.542-0.789) in the validation cohort. Improved performance was achieved by adding Rad-score to the clinical factors. The AUCs of the combined model (0.828; 95%CI: 0.774-0.873 in the training cohort and 0.801; 95%CI: 0.679-0.892 in the validation cohort) were higher than those of the clinical model ($P < 0.001$ and $P = 0.045$, respectively), as shown in Table 3 and Figure 5. The combined model had a higher AUC than Rad-score (AUC = 0.828 vs 0.760, $P = 0.020$) in the training cohort. However, there was no significant difference between the combined model and Rad-score in the validation cohort (AUC = 0.801 vs 0.782, $P = 0.640$).

Table 3 Comparisons of variables and models in the training and validation cohorts

	The training set				The validation set			
	AUC	SEN (%)	SPE (%)	P value	AUC	SEN (%)	SPE (%)	P value
CEA	0.597 (0.533-0.660)	50.00	76.38	< 0.001	0.635 (0.502-0.754)	96.55	40.63	0.042
cT stage	0.613 (0.549-0.675)	84.35	33.86	< 0.001	0.589 (0.456-0.714)	75.86	43.75	0.004
cN stage	0.670 (0.607-0.729)	42.61	84.25	< 0.001	0.684 (0.553-0.797)	86.21	40.63	0.045
Rad-score	0.760 (0.701-0.812)	72.17	69.29	0.020	0.782 (0.658-0.878)	68.97	78.12	0.640
Clinical model	0.718 (0.657-0.774)	63.48	70.08	< 0.001	0.674 (0.542-0.789)	65.52	71.87	0.045
Combined model	0.828 (0.774-0.873)	66.09	88.19		0.801 (0.679-0.892)	62.07	93.75	

P value: Compared with the combined model by DeLong's test. AUC: Area under the receiver operating characteristic curve; SEN: Sensitivity; SPE: Specificity; CEA: Carcinoembryonic antigen.

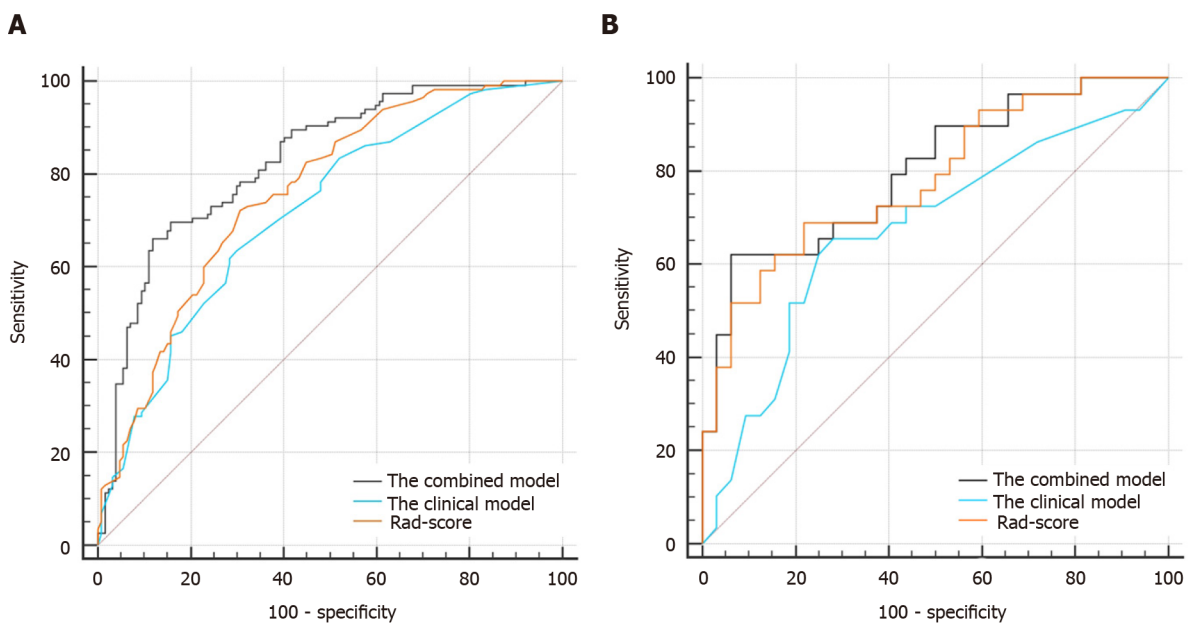


Figure 5 The comparisons of receiver operating characteristic curves in this study. A: In the training cohort: Area under the receiver operating characteristic curve (AUC) = 0.828 for the combined model, 0.718 for the clinical model, and 0.760 for Rad-score; B: In the validation cohort: AUC = 0.801 for the combined model, 0.674 for the clinical model, and 0.782 for Rad-score.

Subgroup analysis

In the cohort of patients treated with nCRT, the AUC of the combined model was higher than that of the clinical model (AUC = 0.853 *vs* 0.710, $P = 0.011$) (Table 4). Among stage III patients, the combined model still had a higher AUC than the clinical model (AUC = 0.796 *vs* 0.630, $P < 0.001$). As for the performance among stage II patients, the combined model failed to outperform the clinical model (AUC = 0.670 *vs* 0.553, $P = 0.098$). Considering the difference between the upper third RC and middle-lower RC in prognosis[23], we performed a subgroup analysis showing that the AUC of the combined model in upper RC group (0.817; 95%CI: 0.730-0.885) was similar with that of the middle-lower RC group (0.824; 95%CI: 0.764-0.875).

DISCUSSION

In this study, a combined model showing potential for predicting PNI of RC outperformed the clinical model (AUC = 0.828 *vs* 0.718, $P < 0.001$ in the training cohort; 0.801 *vs* 0.674, $P = 0.045$ in the validation cohort), indicating that adding Rad-score to the clinical factors improved the predictive value. However, model calibration was not perfect due to the modest overestimation of PNI risk for high-risk patients.

Table 4 Subgroup analyses of the models in the whole cohort

Subgroups	The clinical model			The combined model			P value
	AUC	SEN (%)	SPE (%)	AUC	SEN (%)	SPE (%)	
nCRT							
With (<i>n</i> = 62)	0.710 (0.581-0.818)	68.00	75.68	0.853 (0.740-0.930)	68.00	89.19	0.011
Without (<i>n</i> = 241)	0.712 (0.650-0.768)	48.74	83.61	0.814 (0.759-0.861)	65.55	87.70	< 0.001
Stage							
II (<i>n</i> = 62)	0.553 (0.422-0.680)	21.05	93.02	0.670 (0.538-0.784)	36.84	100.00	0.098
III (<i>n</i> = 193)	0.630 (0.558-0.698)	56.52	69.23	0.796 (0.732-0.851)	73.04	79.49	< 0.001

P value: Comparisons between the clinical model and combined model. AUC: Area under the receiver operating characteristic curve; SEN: Sensitivity; SPE: Specificity; nCRT: Neoadjuvant chemoradiotherapy.

It has been shown in recent studies that PNI is not only the simple diffusion of cancer cells along connective tissues covering the nerve sheath, but also the interaction of a variety of neurotrophic factors and chemokines between cancer cells and the surrounding microenvironment[5,6]. This process may induce cancer invasion, local recurrence, and metastasis, resulting in poor prognosis. Accurate prediction of PNI helps to evaluate prognosis of RC patients. Currently, the sole approach to determine PNI status is the pathological examination of surgical specimens. Preoperative prediction of PNI helps the formulation of individualized treatment[16,24]. For example, PNI⁺ patients should accept more aggressive treatment; for instance, nCRT.

In contrast to CT and MRI, radiomics may achieve desirable outcomes for predicting PNI by extracting high-throughput features that can quantify differences between tissues invisible to the naked eyes. Different MRI-based radiomics models have been reported in RC[6,17,18]. However, the sample sizes in the previous studies were small (PNI⁺: 26-32). In our study, a total of 144 PNI⁺ patients were enrolled, which increased the reliability of the conclusion.

As for the methodology of radiomics, the machine-learning methods used in our study and previous studies were similar. However, the previous studies only included the intratumoral region, ignoring the peritumoral region in which PNI can also appear [7]. There is evidence that radiomics features of peritumoral regions can offer information about biological characteristics of other tumors, such as gastric[25], breast [26], and lung[27] cancer. Different from the previous studies[6,17,18], we built the model by using both peri- and intratumoral regions, and the model had comparable AUCs with the previous MRI-based models[6,18]. The specificities of our model were 88.19% in the training cohort and 93.75% in the validation cohort, as shown in Table 3, indicating low false-positive rate (misdiagnosis rate) for detecting PNI. However, the sensitivities were low (66.09% in the training cohort and 62.07% in the validation cohort).

In terms of clinical factors, cT and cN included in our model revealed a higher risk of PNI in patients with more advanced RC, which was consistent with the conclusion of a meta-analysis[28]. As for Rad-score, it was more important than clinical factors in the prediction of PNI, due to its longer axis in the nomogram. For example, a PNI⁺ lesion in Figure 2 was incorrectly identified as PNI⁻ by the clinical model (CEA = negative, cT = T3, cN = N1a) and correctly determined after adding Rad-score (0.805) to the clinical model with a total score of 12 points in the nomogram, showing a probability of 73% to be PNI⁺.

Referring to the 62 patients receiving nCRT, we found that AUC of the combined model was improved (0.853; 95%CI: 0.740-0.930), suggesting that this model was also suitable for patients treated with nCRT. With the consideration of individualized evaluation of RC patients with different stages, the combined model obtained a higher AUC than the clinical model for stage III patients (AUC = 0.796 *vs* 0.630, *P* < 0.001). However, the combined model failed to outperform the clinical model among stage II patients (AUC = 0.670 *vs* 0.553, *P* = 0.098), which might be caused by the small sample size of stage II patients. As for the subgroup analysis of location, the combined model had similar predictive values in upper RC group (AUC = 0.817) and in middle-lower RC group (AUC = 0.824), indicating good applicability of the model for both upper and middle-lower RC patients.

There were several limitations to this study. Firstly, bias may have existed due to the retrospective design of this study. Secondly, PNI patients from January 2019 to October 2019 were not included, because the current PNI patients were sufficient to complete this radiomics analysis. Thirdly, all patients were enrolled from a single institution. In the future, it is necessary to conduct a multicenter validation to extend the versatility of the radiomics model.

CONCLUSION

A combined model incorporating a radiomics signature and clinical factors was described in this study. This model can provide assistance in the individualized prediction of PNI status in patients with RC.

ARTICLE HIGHLIGHTS

Research background

Perineural invasion (PNI) has emerged as an independent prognostic factor in patients with rectal cancer (RC). The preoperative prediction of PNI status is beneficial for individualized treatment and improved prognosis.

Research motivation

Nowadays, preoperative assessment of PNI status is still challenging.

Research objectives

To build a radiomics prediction model for evaluating PNI status preoperatively in RC patients.

Research methods

We enrolled 303 RC patients in a single institution from March 2018 to October 2019. These patients were classified as the training cohort ($n = 242$) and validation cohort ($n = 61$). A large number of intra- and peritumoral radiomics features were extracted to build the Rad-score and combined model.

Research results

Our study enrolled more patients (144 PNI⁺ and 159 PNI⁻) than previous studies[6,17, 18]. Rad-score was built by logistic regression analysis. The combined model was developed by combining Rad-score with computed tomography (CT)-reported T stage and N stage, and carcinoembryonic antigen. The combined model showed good performance to predict PNI status, with an area under the receiver operating characteristic curve of 0.828 [95% confidence interval (CI): 0.774-0.873] in the training cohort and 0.801 (95%CI: 0.679-0.892) in the validation cohort.

Research conclusions

The combined model incorporating Rad-score and clinical factors helps to provide an individualized PNI status evaluation.

Research perspectives

Other biological characteristics besides PNI are also related to the prognosis of RC patients; for instance, intramural lymphovascular invasion (LVI). Intramural LVI cannot be determined by magnetic resonance imaging and CT. Therefore, using radiomics or deep learning to predict intramural LVI of RC is valuable in the future.

REFERENCES

- 1 Siegel RL, Miller KD, Goding Sauer A, Fedewa SA, Butterly LF, Anderson JC, Cercek A, Smith RA, Jemal A. Colorectal cancer statistics, 2020. *CA Cancer J Clin* 2020; **70**: 145-164 [PMID: 32133645 DOI: 10.3322/caac.21601]
- 2 Lombardi R, Cuicchi D, Pinto C, Di Fabio F, Iacopino B, Neri S, Tardio ML, Ceccarelli C, Lecce F, Ugolini G, Pini S, Di Tullio P, Taffurelli M, Minni F, Martoni A, Cola B. Clinically-staged T3N0 rectal cancer: is preoperative chemoradiotherapy the optimal treatment? *Ann Surg Oncol* 2010; **17**:

- 838-845 [PMID: 20012700 DOI: 10.1245/s10434-009-0796-7]
- 3 **Meng X**, Xia W, Xie P, Zhang R, Li W, Wang M, Xiong F, Liu Y, Fan X, Xie Y, Wan X, Zhu K, Shan H, Wang L, Gao X. Preoperative radiomic signature based on multiparametric magnetic resonance imaging for noninvasive evaluation of biological characteristics in rectal cancer. *Eur Radiol* 2019; **29**: 3200-3209 [PMID: 30413959 DOI: 10.1007/s00330-018-5763-x]
 - 4 **Kim CH**, Yeom SS, Lee SY, Kim HR, Kim YJ, Lee KH, Lee JH. Prognostic Impact of Perineural Invasion in Rectal Cancer After Neoadjuvant Chemoradiotherapy. *World J Surg* 2019; **43**: 260-272 [PMID: 30151676 DOI: 10.1007/s00268-018-4774-8]
 - 5 **Liebig C**, Ayala G, Wilks JA, Berger DH, Albo D. Perineural invasion in cancer: a review of the literature. *Cancer* 2009; **115**: 3379-3391 [PMID: 19484787 DOI: 10.1002/encr.24396]
 - 6 **Chen J**, Chen Y, Zheng D, Pang P, Zhang H, Zheng X, Liao J. Pretreatment MR-based radiomics nomogram as potential imaging biomarker for individualized assessment of perineural invasion status in rectal cancer. *Abdom Radiol (NY)* 2021; **46**: 847-857 [PMID: 32870349 DOI: 10.1007/s00261-020-02710-4]
 - 7 **Ueno H**, Hase K, Mochizuki H. Criteria for extramural perineural invasion as a prognostic factor in rectal cancer. *Br J Surg* 2001; **88**: 994-1000 [PMID: 11442534 DOI: 10.1046/j.0007-1323.2001.01810.x]
 - 8 **Ceyhan GO**, Liebl F, Maak M, Schuster T, Becker K, Langer R, Demir IE, Hartel M, Friess H, Rosenberg R. The severity of neural invasion is a crucial prognostic factor in rectal cancer independent of neoadjuvant radiochemotherapy. *Ann Surg* 2010; **252**: 797-804 [PMID: 21037435 DOI: 10.1097/SLA.0b013e3181fcab8d]
 - 9 **Sun Q**, Liu T, Liu P, Luo J, Zhang N, Lu K, Ju H, Zhu Y, Wu W, Zhang L, Fan Y, Liu Y, Li D, Liu L. Perineural and lymphovascular invasion predicts for poor prognosis in locally advanced rectal cancer after neoadjuvant chemoradiotherapy and surgery. *J Cancer* 2019; **10**: 2243-2249 [PMID: 31258728 DOI: 10.7150/jca.31473]
 - 10 **Peng J**, Sheng W, Huang D, Venook AP, Xu Y, Guan Z, Cai S. Perineural invasion in pT3N0 rectal cancer: the incidence and its prognostic effect. *Cancer* 2011; **117**: 1415-1421 [PMID: 21425141 DOI: 10.1002/encr.25620]
 - 11 **Huang CM**, Huang CW, Huang MY, Lin CH, Chen CF, Yeh YS, Ma CJ, Huang CJ, Wang JY. Coexistence of perineural invasion and lymph node metastases is a poor prognostic factor in patients with locally advanced rectal cancer after preoperative chemoradiotherapy followed by radical resection and adjuvant chemotherapy. *Med Princ Pract* 2014; **23**: 465-470 [PMID: 25012611 DOI: 10.1159/000363604]
 - 12 **Nikberg M**, Chabok A, Letocha H, Kindler C, Glimelius B, Smedh K. Lymphovascular and perineural invasion in stage II rectal cancer: a report from the Swedish colorectal cancer registry. *Acta Oncol* 2016; **55**: 1418-1424 [PMID: 27732105 DOI: 10.1080/0284186X.2016.1230274]
 - 13 **Song JH**, Yu M, Kang KM, Lee JH, Kim SH, Nam TK, Jeong JU, Jang HS, Lee JW, Jung JH. Significance of perineural and lymphovascular invasion in locally advanced rectal cancer treated by preoperative chemoradiotherapy and radical surgery: Can perineural invasion be an indication of adjuvant chemotherapy? *Radiother Oncol* 2019; **133**: 125-131 [PMID: 30935568 DOI: 10.1016/j.radonc.2019.01.002]
 - 14 **Huang Y**, He L, Dong D, Yang C, Liang C, Chen X, Ma Z, Huang X, Yao S, Tian J, Liu Z. Individualized prediction of perineural invasion in colorectal cancer: development and validation of a radiomics prediction model. *Chin J Cancer Res* 2018; **30**: 40-50 [PMID: 29545718 DOI: 10.21147/j.issn.1000-9604.2018.01.05]
 - 15 **Huang X**, Liu J, Wu G, Chen S, Pe FJ, Xie W, Tang W. Development and Validation of a Nomogram for Preoperative Prediction of Perineural Invasion in Colorectal Cancer. *Med Sci Monit* 2019; **25**: 1709-1717 [PMID: 30837449 DOI: 10.12659/MSM.914900]
 - 16 **Yang Y**, Huang X, Sun J, Gao P, Song Y, Chen X, Zhao J, Wang Z. Prognostic value of perineural invasion in colorectal cancer: a meta-analysis. *J Gastrointest Surg* 2015; **19**: 1113-1122 [PMID: 25663635 DOI: 10.1007/s11605-015-2761-z]
 - 17 **Guo Y**, Wang Q, Guo Y, Zhang Y, Fu Y, Zhang H. Preoperative prediction of perineural invasion with multi-modality radiomics in rectal cancer. *Sci Rep* 2021; **11**: 9429 [PMID: 33941817 DOI: 10.1038/s41598-021-88831-2]
 - 18 **Yang YS**, Qiu YJ, Zheng GH, Gong HP, Ge YQ, Zhang YF, Feng F, Wang YT. High resolution MRI-based radiomic nomogram in predicting perineural invasion in rectal cancer. *Cancer Imaging* 2021; **21**: 40 [PMID: 34039436 DOI: 10.1186/s40644-021-00408-4]
 - 19 **Bakst RL**, Wong RJ. Mechanisms of Perineural Invasion. *J Neurol Surg B Skull Base* 2016; **77**: 96-106 [PMID: 27123385 DOI: 10.1055/s-0036-1571835]
 - 20 **Benchoufi M**, Matzner-Lober E, Molinari N, Jannot AS, Soyer P. Interobserver agreement issues in radiology. *Diagn Interv Imaging* 2020; **101**: 639-641 [PMID: 32958434 DOI: 10.1016/j.diii.2020.09.001]
 - 21 **van Griethuysen JJM**, Fedorov A, Parmar C, Hosny A, Aucoin N, Narayan V, Beets-Tan RGH, Fillion-Robin JC, Pieper S, Aerts HJWL. Computational Radiomics System to Decode the Radiographic Phenotype. *Cancer Res* 2017; **77**: e104-e107 [PMID: 29092951 DOI: 10.1158/0008-5472.CAN-17-0339]
 - 22 **Roldán-Nofuentes JA**, Amro RM. Combination of the weighted kappa coefficients of two binary diagnostic tests. *J Biopharm Stat* 2018; **28**: 909-926 [PMID: 29172996 DOI: 10.1080/10543406.2017.1402781]

- 23 **Clancy C**, Flanagan M, Marinello F, O'Neill BD, McNamara D, Burke JP. Comparative Oncologic Outcomes of Upper Third Rectal Cancers: A Meta-analysis. *Clin Colorectal Cancer* 2019; **18**: e361-e367 [PMID: 31445919 DOI: 10.1016/j.clcc.2019.07.004]
- 24 **Cienfuegos JA**, Rotellar F, Baixauli J, Beorlegui C, Sola JJ, Arbea L, Pastor C, Arredondo J, Hernández-Lizoáin JL. Impact of perineural and lymphovascular invasion on oncological outcomes in rectal cancer treated with neoadjuvant chemoradiotherapy and surgery. *Ann Surg Oncol* 2015; **22**: 916-923 [PMID: 25190129 DOI: 10.1245/s10434-014-4051-5]
- 25 **Jiang Y**, Wang H, Wu J, Chen C, Yuan Q, Huang W, Li T, Xi S, Hu Y, Zhou Z, Xu Y, Li G, Li R. Noninvasive imaging evaluation of tumor immune microenvironment to predict outcomes in gastric cancer. *Ann Oncol* 2020; **31**: 760-768 [PMID: 32240794 DOI: 10.1016/j.annonc.2020.03.295]
- 26 **Braman N**, Prasanna P, Whitney J, Singh S, Beig N, Etesami M, Bates DDB, Gallagher K, Bloch BN, Vulchi M, Turk P, Bera K, Abraham J, Sikov WM, Somlo G, Harris LN, Gilmore H, Plecha D, Varadan V, Madabhushi A. Association of Peritumoral Radiomics With Tumor Biology and Pathologic Response to Preoperative Targeted Therapy for HER2 (ERBB2)-Positive Breast Cancer. *JAMA Netw Open* 2019; **2**: e192561 [PMID: 31002322 DOI: 10.1001/jamanetworkopen.2019.2561]
- 27 **Pérez-Morales J**, Tunali I, Stringfield O, Eschrich SA, Balagurunathan Y, Gillies RJ, Schabath MB. Peritumoral and intratumoral radiomic features predict survival outcomes among patients diagnosed in lung cancer screening. *Sci Rep* 2020; **10**: 10528 [PMID: 32601340 DOI: 10.1038/s41598-020-67378-8]
- 28 **Knijn N**, Mogk SC, Teerenstra S, Simmer F, Nagtegaal ID. Perineural Invasion is a Strong Prognostic Factor in Colorectal Cancer: A Systematic Review. *Am J Surg Pathol* 2016; **40**: 103-112 [PMID: 26426380 DOI: 10.1097/PAS.0000000000000518]



Published by **Baishideng Publishing Group Inc**
7041 Koll Center Parkway, Suite 160, Pleasanton, CA 94566, USA
Telephone: +1-925-3991568
E-mail: bpgoffice@wjgnet.com
Help Desk: <https://www.f6publishing.com/helpdesk>
<https://www.wjgnet.com>

